Cr^{3+} in pure and Mg-doped $LiNbO_3$: analysis of the EPR and optical spectra

1992 J. Phys.: Condens. Matter 4 847

(http://iopscience.iop.org/0953-8984/4/3/023)

J. Phys.: Condens. Matter 4 (1992) 847–853. Printed in the UK

Cr^{3+} in pure and Mg-doped $LiNbO_3$: analysis of the EPR and optical spectra

A Martín†, F J López and F Agulló-López
Departamento de Física Aplicada, C-IV, Universidad Autónoma de Madrid, Cantoblanco, E-28049 Madrid, Spain

Received 12 August 1991

Abstract. The electron paramagnetic resonance spectra of Cr^{3+} in $LiNbO_3$ and heavily Mg-doped $LiNbO_3$, have been measured and analysed according to the superposition model. The axial spectrum of Cr^{3+} in $LiNbO_3$ is consistent with Nb substitution. On the other hand, the dominant isotropic spectrum found in Mg-doped $LiNbO_3$ can be accounted for if an appropriate ($\approx$0.1 Å) relaxation of the Cr^{3+} along the c-axis is allowed. Moreover, a point-ion calculation shows that the axial shift of the impurity ion is also qualitatively consistent with recent observations of an enhanced π-polarization character of the optical transitions in $LiNbO_3$: Mg, Cr.

1. Introduction

There is a growing interest in the characterization of transition-metal and rare-earth impurities in $LiNbO_3$ crystals because of their relevance to optoelectronic applications [1, 2]. Unfortunately, $LiNbO_3$ is markedly susceptible to laser damage through the so-called photorefractive effect [3], i.e. light-induced change in the refractive index. However, it has been reported [4] that the addition of 4.6% Mg to $LiNbO_3$ strongly enhances the damage resistance, and so opens the way to the successful operation of stable laser systems. In particular, laser action as recently reported [5] for $LiNbO_3$: Mg, Nd may exploit the electrooptic and non-linear properties of $LiNbO_3$, allowing for Q-switching and frequency doubling in the same active crystal. In this context, Cr^{3+} is an interesting ion which has been successfully used for laser emission in various crystal hosts. Moreover, the broad $^4T_2 \rightarrow {}^4A_2$ emission band (770–1170 nm) reported for $LiNbO_3$ [6] would permit a very wide range of frequency tunability.

The electron paramagnetic resonance (EPR) of $LiNbO_3$: Cr crystals shows an intense axial spectrum attributed to Cr^{3+} substituting for Nb [7] and designated hereon as Cr^{3+}(Nb). This assignment is in agreement with theoretical calculations for the energy levels [8]. However, this simple picture may not be complete, since some low-intensity non-axial EPR spectra have also been observed [9] and evidence for compensating dimers Cr^{3+}(Nb)–Cr^{3+}(Li) has been obtained from EPR [9, 10] and optical spectroscopy [11].

† Permanent address: Departamento de Física e Instalaciones, ETS de Arquitectura, Universidad Politécnica de Madrid, Avda. Juan de Herrera 4, E-28040 Madrid, Spain.

0953-8984/92/030847 + 07 $03.50

The effect of heavy Mg-doping on Cr^{3+} spectra has been the object of very recent work. On one side, a new isotropic EPR line has been detected and associated to Cr^{3+} at Nb sites from ENDOR measurements [12]. From this result, authors proposed that the previously reported axial spectrum in $LiNbO_3$:Cr should be assigned to Cr^{3+} at Li sites, i.e. to Cr^{3+}(Li). On the other hand, a detailed optical spectroscopy study of Mg- and Cr-doped samples [13, 14] has shown new absorption and emission spectra induced by the presence of Mg. These spectra correspond to a Cr-centre in an axial crystal field of lower intensity than that for single-doped samples. The new spectra present a much stronger π-polarization character, presumably associated with a reduction of local symmetry from C_{3v} to C_3. Unfortunately, no explanation has been offered for the apparent contradiction between the EPR and optical results.

In this work we have measured the EPR spectra of both $LiNbO_3$:Cr and $LiNbO_3$:Mg, Cr. For the latter system, data were taken on the *same* samples as used in [13, 14] in order to ascertain that the optical spectra reported in [13, 14] and the isotropic EPR line belong to the same centre. The EPR spectra of Cr^{3+} in $LiNbO_3$ and $LiNbO_3$:Mg have been analysed with the superposition model. The analysis is consistent with Cr^{3+} lying at the Nb site in the single- and double-doped samples. However, in $LiNbO_3$:Mg, Cr the impurity is shifted ≈ 0.1 Å along the c-axis towards the centre of the oxygen octahedron, leading to a cancellation of the D axial parameter of the effective spin Hamiltonian. Moreover, a point-ion calculation of the crystal field shows that the shift is also qualitatively consistent with the observed features in the optical spectra of $LiNbO_3$:Mg, Cr.

2. Experimental procedure

The $LiNbO_3$:Cr and $LiNbO_3$:Mg, Cr crystals were grown by the Czochralski method from grade I Johnson–Matthey powder. The $LiNbO_3$:Cr crystals had a Cr/Nb concentration ratio of 0.5% in the melt, while the $LiNbO_3$:Mg, Cr crystals had 6% Mg/Nb and 0.1% Cr/Nb concentration ratios in the melt. The single- and double-doped crystals were uniformly green and pink in colour respectively. The samples were oriented by x-ray diffraction.

The EPR spectra were obtained with a Varian E-12 spectrometer in the X band with a field modulation frequency of 100 kHz at room temperature. Accurate values of the resonance magnetic fields and microwave frequencies were measured with a Bruker NMR gaussmeter (model ER 035 M) and a Hewlett–Packard frequency meter (model 5342A) respectively. The sample was placed in a home-made two-axis goniometer, so it could be rotated in two perpendicular planes.

3. EPR results and discussion

Figure 1 shows the room-temperature spectra of $LiNbO_3$:Cr and $LiNbO_3$:Mg, Cr samples. The single-doped sample shows the previously reported anisotropic spectrum of Cr^{3+} with axial symmetry [7]. No clear evidence for other spectra was obtained. The double-doped sample presents a very weak contribution of the above spectrum and a new very intense isotropic line with $g = 1.971$ as recently reported [12]. This isotropic line can be associated to a Cr^{3+} centre whose D parameter in the spin Hamiltonian is

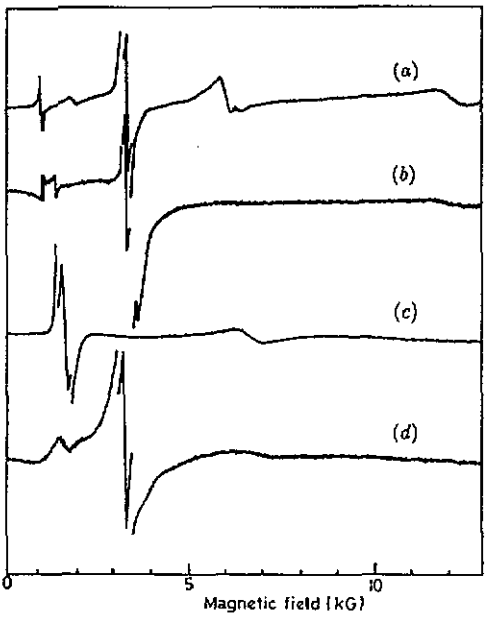

Figure 1. EPR spectra of (*a*), (*c*) $LiNbO_3$: Cr and (*b*), (*d*), $LiNbO_3$: Mg, Cr, measured at room temperature with the magnetic field (*a*), (*b*) parallel to the *c* axis and (*c*), (*d*) perpendicular to the *c* axis. The most intense part of each spectrum has been divided by ten.

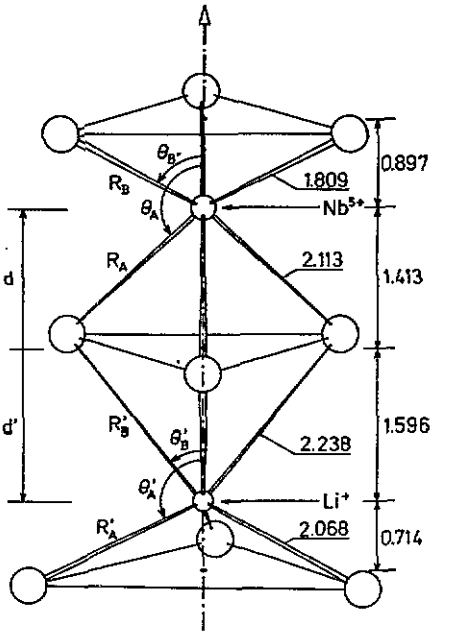

Figure 2. Scheme of the $LiNbO_3$ lattice. On the right side the distances (in Å) for the perfect lattice from Nb^{5+} and Li^+ to the nearest O^{2-} are shown, as well as the distances to the oxygen planes. On the left side, the coordinates (R, θ) of the ligands of the Cr^{3+} impurity substituting for Nb or Li are shown. Here, the sub-index A has been used for ions in the lower plane and sub-index B for ions in the upper plane; also the coordinates with prime refer to the Li site. Those coordinates are expressed as a function of the parameter *d* for Cr^{3+}(Nb) or *d'* for Cr^{3+}(Li).

null. However, this does not mean that the local environment of the Cr^{3+} ion has cubic symmetry, as we will discuss next.

The ^4F ground free-ion term of Cr^{3+} splits into $^4A_2$, $^4T_2$ and $^4T_1$ states in octahedral symmetry and the ^2G term splits into various levels, the ^2E being the lowest of these. If the octahedron is trigonally distorted, there is a first-order splitting of the $^4T_2(^4F)$ and $^4T_1(^4F)$ levels, whereas the $^2E(^2G)$ and $^4A_2(^4F)$ levels split at higher order into 2A and $\bar{E}$ states through a combination of trigonal crystal field distortion and spin–orbit coupling [15]. The states $2\bar{A}(^4A_2)$ and $\bar{E}(^4A_2)$ coming from the ground $^4A_2$ level are the two spin doublets $|\pm\frac{3}{2}\rangle$ and $|\pm\frac{1}{2}\rangle$ observed in EPR spectroscopy whose zero-field separation is usually named $2D$. The transitions from the ground $^4A_2$ level to the $2\bar{A}(^2E)$ and $\bar{E}(^2E)$ levels are the two R-bands detected in optical spectroscopy. The analytical expressions for the energy splittings are:

$$\mathscr{E}[2\bar{A}(^2E)] - \mathscr{E}[\bar{E}(^2E)] = 20.9 \times 10^{-5}\zeta v - 1.1 \times 10^{-5}\zeta v' \quad (1)$$

$$\mathscr{E}[2\bar{A}(^4A_2)] - \mathscr{E}[\bar{E}(^4A_2)] = 2D = -1.44 \times 10^{-8}\zeta^2 v' + 0.09 \times 10^{-8}\zeta^2 v \quad (2)$$

where ζ is the spin–orbit parameter and v and v' are the on- and off-diagonal terms of

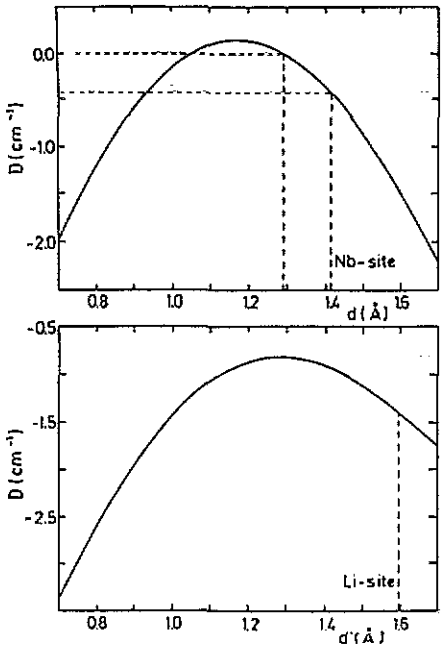

Figure 3. Calculated value of the D parameter as a function of the distance (d or d') from the central oxygen triangle to the Cr^{3+} impurity substituting for Nb (upper part) or Li (lower part).

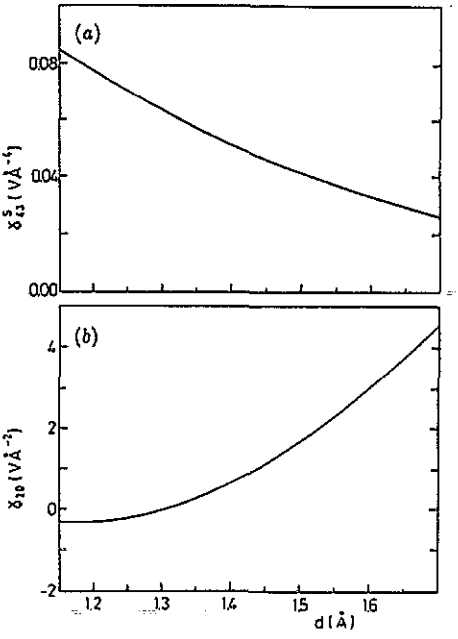

Figure 4. Coefficients (*a*) γ^5_{43} and (*b*) γ_{20} as a function of the distance d from the central oxygen triangle to the Cr^{3+} impurity substituting for Nb.

the trigonal field respectively [16]. As can be seen, the splitting in the ground state is mostly determined by v', while in the ^2E level it is essentially determined by v. Therefore, it is compatible to obtain a splitting in the R bands, indicating a trigonal distortion, and simultaneously, an isotropic EPR line. This would occur if the v' parameter is very small or, if v and v' verify the relation: $v = 16v'$; then $2D$ becomes zero and a single and isotropic line should appear in the EPR spectrum.

In order to gain insight into the structure of the Cr^{3+} centres in both types of sample and to determine the conditions for the occurrence of a centre with trigonal symmetry and $D \approx 0$, the superposition model [17], has been applied. This model assumes that the spin-Hamiltonian parameters can be constructed from the superposition of single-ligand contributions. Since the Cr^{3+} ion has a ^4F ground state, the superposition model as developed for S ground states is not applicable. The appropriate superposition model for Cr^{3+} in a near-cubic environment has already been developed by Newman [18], Clare and Devine [19] and Yeung and Newman [20]. According to these authors the D parameter in the spin Hamiltonian can be expressed as:

$$D = \frac{3}{2}\left(\frac{\zeta}{3\Delta E_2}\right)^2 \sum_l \theta_l \sum_m b_{lm}\langle z(l,m)z\rangle. \tag{3}$$

In this formula, ΔE_2 is the energy of the excited $^4T_2$ level relative to the $^4A_2$ ground state, θ_l represents the Stevens factors $\theta_2 = 2/105$ and $\theta_4 = 2/315$, $\langle z(l,m)z\rangle$ represents the projection coefficients tabulated in [20] and the b_{lm} are given by:

$$b_{lm} = B_{lm} - B_{lm}(\text{cub.}) = \bar{B}_l(R_0)\left[\sum_j \left(\frac{R_0}{R_j}\right)^{t_l} K_l^m(j) - \sum_j K_l^m(j:\text{cub.})\right] \tag{4}$$

where $\bar{B}_l(R_0)$ are the intrinsic parameters $\bar{B}_2$ and $\bar{B}_4$ for a fixed reference distance R_0 and the sum extends to the various ligand ions j whose polar co-ordinates are $(R_j, \theta_j, \varphi_j)$ in a reference system with origin at the impurity. t_l (t_2 and t_4) are the power-law exponents for the dependence on the distance of the intrinsic parameters and K_l^m are the angular coordination factors:

$$K_l^m(\theta_j, \varphi_j) = \sqrt{4\pi/(2l+1)}\, Y_l^{*m}(\theta_j, \varphi_j). \tag{5}$$

Since the impurity may be expected to shift from the exact host-ion location, while keeping trigonal symmetry, the D parameter has been calculated as a function of Cr^{3+} position along the c-axis for both oxygen octahedra around the Nb- and Li-sites. The O^{2-} ions have been assumed to remain in their regular lattice positions [21] shown in figure 2. The distance and angles appearing in (4) and (5), also shown in the figure, have been expressed as a function of a single parameter, d, measuring the position of the impurity along the c-axis from the oxygen plane lying between Nb- and Li-sites. The values for the intrinsic parameters have been taken from [20] and the value of $(\zeta/3\Delta E_2)^2$ has been taken as 2.34×10^{-5} [11, 13]. The results of the calculation are shown in figure 3.

From figure 3, it can be observed that the experimental value of D for $LiNbO_3:Cr^{3+}$ crystals ($-0.41\ cm^{-1}$) [7, 9] is consistent with Cr^{3+} substituting at approximately the Nb position i.e. Cr^{3+}(Nb). On the contrary, it differs considerably from the value corresponding to Li-substitution, i.e. Cr^{3+}(Li). This result suggests that Cr^{3+} occupies the Nb site and supports the original location assignment [7]. It is also in accordance with theoretical calculations using the X_α method [8]. For samples co-doped with Mg, the isotropic line can be expected if the Cr^{3+}(Nb) is allowed to shift 0.12 Å along the c-axis towards the centre, since for this position the calculation shows the cancellation of the D parameter. It is remarkable that the magnitude of the shift is the same as has been estimated from ENDOR measurements [12]. The displacement of Cr^{3+} would be originated by the presence of Mg^{2+} ions at some nearby locations as suggested by ENDOR [12] and optical [14] measurements. On the other hand, it is to be noted from figure 3 that the cancellation of D cannot be obtained if Cr^{3+} lies inside the Li-octahedron, Cr^{3+}(Li).

4. Comparison with optical results

In order to have a coherent picture of the available Cr^{3+} data, it should now be explained that for $LiNbO_3$: Mg, Cr the optical transitions show a strong π-polarization character, in accordance with the local symmetry departing from near C_{3v} to C_3. Although a rigorous quantitative discussion cannot be made, one can offer a simple qualitative argument to justify this effect. The C_3 symmetry in $LiNbO_3$ structure arises from the rotation by an angle α between the two oxygen triangles perpendicular to the c-axis forming the trigonally-deformed octahedron. Therefore the C_3 contribution to the local symmetry will be reinforced when the impurity moves away from either of the oxygen triangles. In fact, when the potential associated to one of the triangles is dominant, the C_{3v} symmetry is approximately obeyed. This trend can now be confirmed by using a

point-ion calculation of the crystal field. The expression of the crystal potential for a d-ion in C_3 symmetry is:

$$V = \gamma_{20} Z_{20}(\theta, \varphi) r^2 + \gamma_{40} Z_{40}(\theta, \varphi) r^4 + \gamma^c_{43} Z^c_{43}(\theta, \varphi) r^4 + \gamma^s_{43} Z^s_{43}(\theta, \varphi) r^4 \tag{6}$$

where the notation of Hutchings [22] for the real tesseral harmonics $Z^{c,s}_{nm}$ and the corresponding coefficients $\gamma^{c,s}_{nm}$ has been used. In the above expression, the term Z^s_{43} is the one responsible for the breaking of C_{3v} symmetry (represented by the term Z^c_{43}) into C_3. So one can calculate the value of the γ^s_{43} coefficient as a function of the position of Cr^{3+} along the c-axis in the octahedron around the Nb site in an analogous way to that used for the calculation of D. The expression for this coefficient reads:

$$\gamma^s_{43} = \frac{4\pi q}{9} \sum_j \frac{Z^s_{43}(\theta_j, \varphi_j)}{R^5_j} \tag{7}$$

with

$$Z^s_{43}(\theta_j, \varphi_j) = \tfrac{3}{8}\sqrt{(70/\pi)} \sin^3 \theta_j \cos \theta_j \sin 3\varphi_j \tag{8}$$

q being the charge on the ligand oxygen ions. The z axis is along the trigonal axis and the x axis is along a binary axis of the closest oxygen triangle (the upper one in figure 2). The rotation angle α between the two triangles has been taken as 41′ for the Nb-octahedron, as inferred from the structural data [21]. The results are shown in figure 4(a). It is clear that the contribution of the C_3 term is smaller near the oxygen planes and increases when the impurity moves towards the centre of the octahedron. So, the shift of Cr^{3+} from the exact Nb-position to that consistent with the isotropic EPR spectrum implies a marked increase of the C_3 symmetry contribution and so it may explain the enhanced π-polarization character of the optical transitions [14]. On the other hand, the second-order axial field, $\gamma_{20} Z_{20} r^2$, can also be calculated within the point-ion approximation (figure 4(b)). This axial contribution decreases when the impurity moves towards the centre of the octahedron. Therefore it would lead (when combined with the spin–orbit interaction) to a reduced ^2E level splitting as experimentally observed [13].

Acknowledgments

The authors wish to acknowledge Professor F Jaque for supplying the samples. This work has been supported by Comisión Interministerial para Ciencia y Tecnología (CICYT) under project MAT88-0431-C02 and fundación Ramón Areces.

References

[1] Agulló-López F and Cabrera J M 1989 *Properties of Lithium Niobate* (*EMIS Datareviews Series 5*) (London: INSPEC) pp 8–17
[2] Schirmer O F, Thiemann O and Wöhlecke M 1991 *J. Phys. Chem. Solids* **52** 185–200
[3] Günter P and Huignard J-P 1988 *Photorefractive Materials and Their Applications I* ed P Günter and J-P Huignard (Berlin: Springer) pp 7–73
[4] Bryan D A, Gerson R and Tomaschke H E 1984 *Appl. Phys. Lett.* **44** 847–9
[5] Fan T Y, Cordova-Plaza A, Digonnet M J F, Byer R L and Shaw H J 1986 *J. Opt. Soc. Am.* B **3** 140–7
[6] Glass A M 1969 *J. Chem. Phys.* **50** 1501–10
[7] Rexford D G, Kim Y M and Story H S 1970 *J. Chem. Phys.* **52** 860–3
[8] Michel-Calendini F M, Moretti P and Chermette H 1987 *Cryst. Latt. Defects Amorph. Mater.* **15** 65–9

[9] Malovichko G I, Grachev V G and Lukin S N 1986 *Sov. Phys.–Solid State* **28** 553–7
[10] Grachev V G, Malovichko G I and Troitskii V V 1987 *Sov. Phys.–Solid State* **29** 349–50
[11] Weiyi J, Huimin L, Knutson R and Yen W M 1990 *Phys. Rev.* B **41** 10 906–10
[12] Corradi G, Söthe H, Spaeth J-M and Polgár K 1991 *J. Phys.: Condens. Matter* **3** 1901–8
[13] Camarillo E, Tocho J, Vergara I, Diéguez E, García-Solé J and Jaque F 1991 *Phys. Rev.* B at press
[14] Camarillo E, García-Solé J, Cussó F, Agulló-López F, Sanz-García J A, Han T P J, Jaque F and Henderson B 1991 *Chem. Phys. Lett.* **185** 505–10
[15] Henderson B and Imbusch G F 1989 *Optical Spectroscopy of Inorganic Solids* (Oxford: Clarendon) pp 410–30
[16] Macfarlane R M 1967 *J. Chem. Phys.* **47** 2066–73
[17] Newman D J and Urban W 1975 *Adv. Phys.* **24** 793–844
[18] Newman D J 1982 *J. Phys. C: Solid State Phys.* **15** 6627–30
[19] Clare J F and Devine S D 1983 *J. Phys. C: Solid State Phys.* **16** 4415–23
[20] Yeung Y Y and Newman D J 1986 *Phys. Rev.* B **34** 2258–65
[21] Abrahams S C and Marsh P 1986 *Acta Crystallogr.* B **42** 61–8
[22] Hutchings M T 1964 *Solid State Physics* vol 16, ed F Seitz and D Turnbull (New York: Academic) pp 227–73